mathematics

MDPI

Article

Monitoring of Linear Profiles Using Linear Mixed Model in the Presence of Measurement Errors

Wenhui Liu, Zhonghua Li * and Zhaojun Wang

School of Statistics and Data Science, LPMC and KLMDASR, Nankai University, Tianjin 300071, China
* Correspondence: zli@nankai.edu.cn

Abstract: In the application of control charts, most of the research in profile monitoring is based on accurate measurements. Measurement errors, however, often exist in many manufacturing and service environments. In this paper, we apply linear mixed models in the presence of measurement errors in fixed effects. We discuss three modified multivariate charts, namely Hotelling's T^2, multivariate exponential weighted moving average (MEWMA) control chart, and multivariate cumulative sum (MCUSUM) control chart. Performance comparisons are made in terms of the average run length (ARL) and average extra quadratic loss (AEQL). Finally, a real data example on healthcare expenditures is used to illustrate the implementation of the proposed monitoring schemes.

Keywords: profile monitoring; measurement errors; linear mixed model; MCUSUM; MEWMA; Hotelling's T^2

MSC: 62P30; 62J05

check for updates

Citation: Liu, W.; Li, Z.; Wang, Z. Monitoring of Linear Profiles Using Linear Mixed Model in the Presence of Measurement Errors. *Mathematics* **2022**, *10*, 4641. https://doi.org/10.3390/math10244641

Academic Editor: Stelios Psarakis

Received: 7 October 2022
Accepted: 6 December 2022
Published: 7 December 2022

1. Introduction

Statistical process control (SPC) has been successfully applied in a variety of industries. In many SPC applications, the quality of a process or product can be characterized and summarized by a relationship between a response variable and one or more explanatory variables, which is referred to as profile [1]. Profile analysis is becoming increasingly prevalent in process monitoring applications due to the rapid recent advances in sensor technology and system automation [2,3].

Analysis of linear profiles has been investigated by a number of authors. The applications of monitoring of simple linear profile can be seen in [1,4–11]. Kazemzadeh et al. [12,13] studied control charts for monitoring of Phase I and II polynomial profiles, respectively. References [14–18] investigated monitoring of multivariate linear profiles. Nonlinear profiles were monitored by [14,19–24]. Jensen et al. [25] presented two T^2 control charts based on a linear mixed model (LMM) for Phase I analysis. Jensen et al. [26] used a nonlinear mixed model to account correlation within nonlinear profiles. Narvand et al. [27] utilized three traditional multivariate control charts to monitor the fixed effects of the auto-correlated LMMs in Phase II. In addition, Soleimani et al. [28] monitored predicted random effects of the LMMs in Phase II and showed that their approaches behaves similarly to the approaches proposed by [27] for monitoring the fixed effects.

Most of the existing research on profile monitoring is based on accurately measured data. However, measurement errors exist in practice and the performance of control charts may be seriously affected [29]. Many scholars have studied the effect of measurement errors on control charts, such as [30–34]. There are very few articles on profile monitoring in the presence of measurement errors. Li and Huang [35] studied regression-based process monitoring with consideration of measurement errors. Wang and Huwang [36] presented three charting schemes for monitoring simple linear Berkson profiles. Noorossana and Zerehsaz [37] discussed the effect of measurement errors on the control charts for Phase II monitoring of simple linear profiles with a random explanatory variable. They provided remedial measures to reduce the effect of measurement errors. The above three articles are based on the error-in-variable (EV) model, which was proposed by Deato [38] in order to correct for the effects of sampling error and is more practical than the ordinary regression model. Linear EV models are commonly used in agronomy, biometrics, education, medicine, and other fields, including extensive monographs [39–42]. For simple linear EV regression models, the asymptotic properties of the least squares (LS) estimators have been studied by many scholars, such as [43–45]. Some scholars have studied the estimation of parameters of LMMs with EV. Profile monitoring of linear mixed models with EV arouses our interest.

In this paper, we focus on a study of Phase II approaches for monitoring linear mixed profile in the presence of measurement errors. The remainder of this paper is organized as follows. In Section 2, we introduce the linear mixed measurement error model (LMMeM) in detail. In Section 3, we present three multivariate control charts to monitor the random effects of LMMeMs in Phase II. We also introduce assessment measures of the proposed charts and the method of seeking control limits in Section 3. Section 4 presents the simulation studies, including the performance results compared with other existing methods. In Section 5, the proposed charts are applied to analyze the healthcare expenditures data. Section 6 provides our conclusions. The detailed estimation procedure is outlined in Appendix A.

2. Methodology

In order to construct Phase II methods for monitoring a simple linear mixed profile in the presence of measurement error, proper models that consider measurement errors are necessary. In this section, we introduce the LMMeM.

2.1. Linear Mixed Measurement Error Model

Denote by $\{(x_{ki}, z_{ki}, y_{ki}), k = 1, 2, \ldots, n; i = 1, 2, \ldots, m\}$ the ith sample collected over time. The profile can be formulated as a general linear mixed measurement error model (LMMeM):

$$\begin{aligned} y_{ki} &= \beta_{0i} + \beta_{1i}\xi_{ki} + b_{0i} + b_{1i}z_{ki} + \varepsilon_{ki}, \\ x_{ki} &= \xi_{ki} + \delta_{ki}. \end{aligned} \tag{1}$$

where independent errors are $\varepsilon_{ki} \sim N(0, \sigma_i^2)$. The random effects are $(b_{0i}, b_{1i})^\top \sim \mathrm{MN}(\mathbf{0}, \mathbf{D})$, where $\mathbf{D}$ is a 2×2 positive definite matrix. x_{ki} is the observed value of z_{ki} with the measurement error δ_{ki}, where δ_{ki} is an random variable from $\mathrm{N}(0, \sigma_\delta^2)$. We assume that $\mathrm{N}(0, \sigma_\delta^2)$ is known. b_{0i}, b_{1i}, δ_{ki}, and ε_{ki} are assumed to be stochastically independent. Rewrite the model (1) in vector–matrix form,

$$\begin{aligned} \mathbf{Y}_i &= \boldsymbol{\xi}_i\boldsymbol{\beta}_i + \mathbf{Z}_i\mathbf{b}_i + \boldsymbol{\varepsilon}_i, \\ \mathbf{X}_i &= \boldsymbol{\xi}_i + \boldsymbol{\delta}_i, \quad i = 1, 2, \ldots, m, \end{aligned} \tag{2}$$

where $\boldsymbol{\delta}_i$ is an $(n \times 2)$ random matrix from $\mathrm{MN}(\mathbf{0}, \mathbf{I}_n \otimes \boldsymbol{\Lambda})$, $\boldsymbol{\Lambda} = \mathrm{diag}(0, \sigma_\delta^2)$.

The null hypothesis of interest is that the process is in control (IC), namely that $\boldsymbol{\beta}_i = \boldsymbol{\beta}$ and $\sigma_i = \sigma$ for all i. The alternative hypothesis is that the process is out of control (OC). The process is initially IC, but after the time point τ, a step shift in the intercept and/or slope and/or standard deviation occurs. Next, we introduce the estimation of fixed and random effects in LMMeM. In this paper, we focus on Phase II of profile monitoring, so we assume that the $\mathbf{D}$ and σ^2 are known or can be estimated well based on IC historical data.

2.2. Estimation of Random Effects

If there is no measurement error, the model in (2) reduces to a standard linear mixed model [46]. The log-likelihood function (omitting a constant term) of $\mathbf{Y}_1, \mathbf{Y}_2, \ldots, \mathbf{Y}_m$ is

$$l(\boldsymbol{\beta}; \boldsymbol{\xi}, Y) = -\frac{1}{2}\log(|\mathbf{V}|) - \frac{1}{2}(\mathbf{Y} - \boldsymbol{\xi}\boldsymbol{\beta})^\top \mathbf{V}^{-1}(\mathbf{Y} - \boldsymbol{\xi}\boldsymbol{\beta}),$$

where $\boldsymbol{\xi}$ is a $(n \times m)$ by 2 stacked matrix of the $\boldsymbol{\xi}_i$'s, $\mathbf{V} = \mathbf{Z}\mathbf{B}\mathbf{Z}^\top + \sigma^2\mathbf{I}_n = \mathrm{diag}(\mathbf{V}_i)$ with $\mathbf{B} = \mathrm{diag}(\mathbf{D})$, $\mathbf{V}_i = \mathbf{Z}_i\mathbf{D}\mathbf{Z}_i^\top + \sigma^2\mathbf{I}_n$, and $\mathbf{Z}$ is a block diagonal matrix containing all the $\mathbf{Z}_i$ matrices. If $\mathbf{D}$ and σ^2 are known, we can obtain the maximum likelihood estimation of $\boldsymbol{\beta}$, that is

$$\hat{\boldsymbol{\beta}} = (\boldsymbol{\xi}^\top \mathbf{V}^{-1}\boldsymbol{\xi})^{-1}(\boldsymbol{\xi}^\top \mathbf{V}^{-1}\mathbf{Y}). \tag{3}$$

Similarly, we have

$$\hat{\mathbf{b}}_i = \mathbf{D}\mathbf{Z}_i^\top \mathbf{V}_i^{-1}(\mathbf{Y}_i - \boldsymbol{\xi}\hat{\boldsymbol{\beta}}).$$

Soleimani et al. [28] used $\hat{\mathbf{b}}_i$ as a statistic for Phase II monitoring.

When the measurement error is not negligible, if we simply replace $\boldsymbol{\xi}_i$ by $\mathbf{X}_i$, then $\hat{\boldsymbol{\beta}}$ and $\hat{\mathbf{b}}_i$ are not consistent in general. For the model (2), Zhong et al. [47] derived the corrected score estimates of fixed and random effects. The corrected log-likelihood function (omitting a constant) of $\mathbf{Y}_1, \mathbf{Y}_2, \ldots, \mathbf{Y}_m$ is

$$l^*(\boldsymbol{\beta}; \mathbf{X}, \mathbf{Y}) = -\frac{1}{2}\log(|\mathbf{V}|) - \frac{1}{2}[(\mathbf{Y} - \mathbf{X}\boldsymbol{\beta})^\top \mathbf{V}^{-1}(\mathbf{Y} - \mathbf{X}\boldsymbol{\beta}) - \mathbf{tr}(\mathbf{V}^{-1})\boldsymbol{\beta}^\top \boldsymbol{\Lambda}\boldsymbol{\beta}].$$

The corrected estimation of $\boldsymbol{\beta}$ is given by

$$\hat{\boldsymbol{\beta}}_c = \left(\mathbf{X}^\top \mathbf{V}^{-1}\mathbf{X} - \mathrm{tr}(\mathbf{V}^{-1})\boldsymbol{\Lambda}\right)^{-1}(\mathbf{X}^\top \mathbf{V}^{-1}\mathbf{Y}) \tag{4}$$

and the corrected estimation of $\mathbf{b}_i$ is

$$\hat{\mathbf{b}}_i = \mathbf{D}\mathbf{Z}_i^\top \mathbf{V}_i^{-1}(\mathbf{Y}_i - \mathbf{X}_i\hat{\boldsymbol{\beta}}_c). \tag{5}$$

As pointed out by [47], under some regularity conditions, the corrected estimations $\hat{\boldsymbol{\beta}}_c$ and $\hat{\mathbf{b}}_i$ are consistent and normally distributed asymptotically.

In practice, $\mathbf{D}$ and σ^2 are not known and therefore must be estimated beforehand. We provide the derivation details in Appendix A.

3. Proposed Control Charts

In this section, we construct Phase II charts for monitoring a linear mixed profile in the presence of measurement errors. We assume that the $\boldsymbol{\beta}$, $\mathbf{D}$, σ^2 are known or can be estimated well based on IC historical data.

We are interested in the predictions of random effects $\hat{\mathbf{b}}_i$ for constructing control charts. If there is no measurement error, Jensen et al. [25] proved that $\sum_{i=1}^n \mathbf{b}_i = \mathbf{0}$ when the $\mathbf{Z}_i$ matrix is contained within the $\boldsymbol{\xi}_i$ matrix. They used $\hat{\mathbf{b}}_i$ to monitor the stability of the process. However, when the measurement error exists, the equation $\sum_{i=1}^n \mathbf{b}_i = \mathbf{0}$ does not hold. We can obtain an estimate of the covariance matrix of $\hat{\mathbf{b}}_i$ from a total of m IC historical data. The mean and variance are obtained as well, respectively,

$$\bar{\mathbf{b}}_{\mathrm{IC}} = \frac{1}{m}\sum_{i=1}^{m}\hat{\mathbf{b}}_i, \tag{6}$$

$$\hat{\boldsymbol{\Sigma}}_{\mathrm{IC}} = \frac{\sum_{i=1}^{m-1}(\hat{\mathbf{b}}_{i+1} - \hat{\mathbf{b}}_i)(\hat{\mathbf{b}}_{i+1} - \hat{\mathbf{b}}_i)^\top}{2(m-1)}, \tag{7}$$

where $\hat{\boldsymbol{\Sigma}}_{\mathrm{IC}}$ represents the successive-differences variance–covariance matrix of the estimated random effects. Sullivan and Woodall [48] suggested using $\hat{\boldsymbol{\Sigma}}_{\mathrm{IC}}$ for improving the ability of the Hotelling's T^2 control chart for detecting the presence of sustained shifts between the profiles.

The estimators of Equations (6) and (7) may break down in presence of outliers in Phase I. Diagnostic methods in LMMeM have been studied by some authors [49–52].

3.1. The Hotelling's T^2 Control Chart

The Hotelling's T^2 statistics, based on the successive differences estimator of the variance–covariance matrix, are

$$T_i^2 = (\hat{\mathbf{b}}_i - \bar{\mathbf{b}}_{\mathrm{IC}})^\top \hat{\boldsymbol{\Sigma}}_{\mathrm{IC}}^{-1} (\hat{\mathbf{b}}_i - \bar{\mathbf{b}}_{\mathrm{IC}}). \tag{8}$$

The chart signals as soon as any T_i^2 exceeds the desired upper control limits (UCL).

3.2. The MEWMA Control Chart

The second approach is to use the MEWMA chart proposed by [53] to monitor any shift in $\hat{\mathbf{b}}_i$, as follows:

$$\mathbf{w}_i = \theta(\hat{\mathbf{b}}_i - \bar{\mathbf{b}}_{\mathrm{IC}}) + (1-\theta)\mathbf{w}_{i-1}, \tag{9}$$

where $\mathbf{w}_0 = \mathbf{0}$ and θ $(0 < \theta < 1)$ is the specified smoothing parameter. Then the MEWMA statistic for the ith profile is calculated as follows:

$$\mathrm{MEWMA}_i = \mathbf{w}_i^\top \boldsymbol{\Sigma}_{\mathbf{w}}^{-1} \mathbf{w}_i, \tag{10}$$

where

$$\boldsymbol{\Sigma}_{\mathbf{w}} = \frac{\theta}{2-\theta} \hat{\boldsymbol{\Sigma}}_{\mathrm{IC}}. \tag{11}$$

This control chart gives a signal when $\mathrm{MEWMA}_i > \mathrm{UCL}$.

3.3. The MCUSUM Control Chart

The third proposed approach is based on the MCUSUM control chart proposed by [54]. The statistic is given by

$$\mathbf{s}_i = \begin{cases} \mathbf{0}; & \text{for } c_i \le c, \\ (\mathbf{s}_{i-1} + \hat{\mathbf{b}}_i - \bar{\mathbf{b}}_{\mathrm{IC}})(1 - c/c_i); & \text{for } c_i > c, \end{cases} \tag{12}$$

where $c_i = [(\mathbf{s}_{i-1} + \hat{\mathbf{b}}_i - \bar{\mathbf{b}}_{\mathrm{IC}})^\top \hat{\Sigma}_{\mathrm{IC}}^{-1} (\mathbf{s}_{i-1} + \hat{\mathbf{b}}_i - \bar{\mathbf{b}}_{\mathrm{IC}})]^{1/2}$, $\mathbf{s}_0 = \mathbf{0}$ and c is a selected constant.

The chart triggers a signal when $(\mathbf{s}_i^\top \hat{\boldsymbol{\Sigma}}_{\mathrm{IC}}^{-1} \mathbf{s}_i)^{1/2} > \mathrm{UCL}$.

3.4. Performance Measures

To assess the performance of control charts, we usually examine the average run length (ARL). ARL reflects the average number of observations plotted on a control chart until the chart triggers an OC signal. ARL is classified as either IC ARL or OC ARL, denoted as ARL_0 and ARL_1, respectively. We fix the ARL_0, then calculate the UCLs to achieve ARL_0. After that, based on the constructed charts, we compute ARL_1 and we expect ARL_1 to be as small as possible.

We also use average extra quadratic loss (AEQL) to evaluate the overall performance of a control chart for a wide range of shifts against other charts. It is defined by

$$\mathrm{AEQL} = \frac{1}{\alpha_{\max} - \alpha_{\min}} \sum_{\alpha_{\max}}^{\alpha_{\min}} \alpha_i^2 \mathrm{ARL}(\alpha_i),$$

where δ_i is defined in $[\alpha_{\min}, \alpha_{\max}]$; the $\alpha_{\max}$ and $\alpha_{\min}$ are known as maximum and minimum values of shift, respectively. A smaller AEQL value for a control chart indicates better overall performance of this control chart.

3.5. Searching UCLs

The desired UCLs for each chart mentioned above can be estimated by the bisection searching algorithm. The desired UCLs for each chart can be performed as follows:

Step 1: The initial values of lower and upper bounds are pre-specified, denoted as UCL_l and UCL_u. It is desirable that $\text{ARL}_l < \text{ARL}_0 < \text{ARL}_u$, where ARL_l and ARL_u are the corresponding ARL values of UCL_l and UCL_u, respectively.

Step 2: Let $\text{UCL}_{iter} = (\text{UCL}_l + \text{UCL}_u)/2$ and ARL_{iter} be the corresponding ARL value. If $\text{ARL}_{iter} < \text{ARL}_0$, then assign $\text{UCL}_l = \text{UCL}_{iter}$ and $\text{ARL}_l = \text{ARL}_{iter}$. Otherwise, assign $\text{UCL}_u = \text{UCL}_{iter}$ and $\text{ARL}_u = \text{ARL}_{iter}$.

Step 3: Repeat Step 2 until $|\text{ARL}_u - \text{ARL}_l|$ is sufficiently small and then the desired $\text{UCL} = (\text{UCL}_l + \text{UCL}_u)/2$ is obtained.

We use the above bisection searching algorithm to find the UCLs for the proposed charts under different measurement errors.

4. Performance Study

In this section, we provide the performance evaluations of the proposed charts. We also analyze the effect of ignoring measurement error and/or random effects on the performance of control charts.

To demonstrate the performance of the proposed approaches, consider the underlying LMMeM:

$$\begin{aligned} y_{ki} &= 3 + 2\xi_k + b_{0i} + b_{1i}z_k + \varepsilon_{ki}, \\ x_{ki} &= \xi_k + \delta_{ki}, i = 1, 2, \ldots, m, \end{aligned}$$

where $\xi = z = 2, 4, 6, 8$, $\delta_{kj} \sim N(0, \sigma_\delta^2)$, $\varepsilon_{ki} \sim N(0, 1)$ and $(b_{0i}, b_{1i})^\top \sim \text{MN}(\mathbf{0}, \mathbf{D})$ with

$$\mathbf{D} = \begin{pmatrix} d_1^2 & \rho d_1 d_2 \\ \rho d_1 d_2 & d_2^2 \end{pmatrix}.$$

We set $d_1^2 = d_2^2 = 0.1$, $\rho = 0, 0.1, 0.5, 0.9$, and $m = 1000$.

The overall IC ARL is roughly set to 200, then 20,000 simulation runs were conducted for each chart to search the UCLs. The OC ARL values were evaluated through the use of 20,000 simulation runs under different shifts in intercept, slope, and standard deviation. For MCUSUM and MEWMA charts, the choices of parameters are $c = 0.5$—as suggested by [55]—and $\theta = 0.2$, respectively. The simulated UCLs values for three proposed control charts are presented in Table 1.

Table 1. The UCL values for three proposed control charts when $\text{ARL}_0 \simeq 200$.

σ_δ^2	T^2				MEWMA				MCUSUM			
	0.0	**0.1**	**0.5**	**0.9**	**0.0**	**0.1**	**0.5**	**0.9**	**0.0**	**0.1**	**0.5**	**0.9**
0.00	10.762	11.255	9.590	10.890	9.918	10.251	8.731	10.468	5.653	5.791	5.021	6.060
0.01	10.309	9.700	11.018	11.563	10.815	9.003	10.132	10.610	6.170	5.175	5.748	5.987
0.04	10.594	11.618	10.739	12.726	9.646	10.678	9.947	11.555	5.468	6.008	6.015	6.407
0.09	9.727	11.811	10.829	12.032	8.871	11.093	10.201	10.938	5.110	6.315	5.841	6.086

Control charts were compared at both zero-state and steady-state. In zero-state, the shift is assumed to occur at the beginning of the process. In steady-state, the process has been operating for some time τ before a process shift occurs. We set $\tau = 25$. Since both MCUSUM and MEWMA charts are not memoryless, in contrast to Hotelling T^2, we compare their performance at zero-state ARL and steady-state ARL. Results are presented in Figures 1–3.

From the above three figures, it can be seen that there is a common conclusion for MCUSUM and MEWMA charts: no matter which parameter occurs, whether there is a shift drift, and how big the measurement error is, the performance of zero-state ARL for each carts is similar to steady-state ARL. Since the advantage of steady-state ARL is not very significant, we only discuss the performance of zero-state ARL below. The OC ARL appearing below all refer to the zero-state OC ARL.

The OC ARLs of the three competing charts for detecting shifts in λ_0, λ_1, and γ are presented in Tables 2–4, respectively.

Table 2. OC ARLs of control charts for different values of σ_δ^2 and ρ under $\lambda_0\sigma$ in intercept.

		T^2				MEWMA				MCUSUM			
ρ	λ_0	**0.00**	**0.01**	**0.04**	**0.09**	**0.00**	**0.01**	**0.04**	**0.09**	**0.00**	**0.01**	**0.04**	**0.09**
0.0	0.2	179.0	195.2	187.6	183.6	106.2	100.4	129.7	127.8	92.0	82.6	115.1	119.3
	0.4	137.1	165.6	159.0	149.2	48.9	47.4	66.2	61.9	40.5	37.4	52.8	54.0
	0.6	99.5	121.6	124.5	106.7	25.8	25.4	35.0	32.0	22.2	21.1	28.0	28.1
	0.8	69.5	82.6	94.1	75.9	16.0	15.9	20.8	19.4	14.3	14.3	17.6	17.6
	1.0	47.9	55.4	68.1	54.3	11.0	11.1	13.9	13.1	10.6	10.7	12.5	12.4
	1.2	33.3	38.0	49.4	37.7	8.3	8.4	10.2	9.6	8.3	8.6	9.6	9.5
	1.4	23.3	26.0	35.1	26.7	6.7	6.7	7.9	7.6	6.8	7.1	7.9	7.6
	1.6	16.4	18.4	25.3	19.4	5.5	5.6	6.5	6.2	5.9	6.1	6.6	6.4
	1.8	11.9	13.0	18.5	14.3	4.7	4.8	5.5	5.3	5.1	5.3	5.7	5.6
	2.0	8.8	9.5	13.7	10.6	4.1	4.2	4.8	4.6	4.5	4.8	5.1	4.9
	AEQL	183.2	209.6	262.8	208.7	56.9	57.1	69.6	66.2	56.5	57.4	66.1	64.9
0.1	0.2	180.4	190.9	181.0	191.3	118.1	155.3	118.5	152.6	103.1	142.3	101.8	140.1
	0.4	136.2	156.8	148.2	160.0	51.7	73.3	59.0	78.3	43.7	62.2	46.0	63.6
	0.6	95.4	117.7	113.7	122.9	26.8	36.1	31.2	39.8	23.1	30.0	25.1	32.7
	0.8	65.3	82.9	82.3	88.7	16.1	20.6	18.9	23.0	14.7	18.1	16.4	20.1
	1.0	43.8	57.5	59.6	62.7	11.1	13.4	12.8	15.1	10.7	12.5	11.9	14.0
	1.2	29.8	39.8	41.9	44.2	8.3	9.8	9.6	11.0	8.4	9.5	9.3	10.8
	1.4	20.5	27.4	30.0	31.4	6.5	7.5	7.5	8.5	6.8	7.6	7.7	8.7
	1.6	14.8	19.4	21.7	22.6	5.4	6.1	6.2	6.9	5.8	6.3	6.5	7.3
	1.8	10.6	13.9	15.8	16.9	4.6	5.2	5.3	5.7	5.1	5.4	5.7	6.3
	2.0	7.9	10.3	11.8	12.4	4.1	4.5	4.6	5.0	4.5	4.8	5.0	5.5
	AEQL	168.1	216.4	228.7	242.4	56.9	68.6	65.2	75.7	57.1	66.0	63.4	73.9
0.5	0.2	186.4	179.7	181.9	184.1	133.5	118.6	129.8	128.3	122.5	103.7	119.1	117.0
	0.4	157.9	148.6	144.2	148.1	66.7	57.8	62.4	64.8	57.2	46.9	53.9	54.8
	0.6	122.8	110.1	104.9	109.6	35.9	30.9	32.6	35.1	29.5	25.4	28.3	29.6
	0.8	92.8	81.5	74.1	80.7	21.1	18.8	19.6	21.5	18.2	16.5	17.9	19.0
	1.0	66.4	58.3	51.2	57.7	13.9	12.8	13.3	14.6	12.8	12.0	12.6	13.6
	1.2	48.3	41.9	36.0	41.6	10.3	9.6	9.8	10.7	9.7	9.4	9.7	10.5
	1.4	34.1	29.9	25.6	29.9	8.0	7.6	7.7	8.4	7.9	7.6	7.9	8.5
	1.6	24.5	21.6	18.9	21.8	6.5	6.2	6.3	6.8	6.6	6.5	6.6	7.2
	1.8	18.0	15.8	13.6	16.3	5.5	5.3	5.3	5.8	5.7	5.7	5.7	6.2
	2.0	13.2	11.7	10.3	12.4	4.8	4.6	4.6	5.0	5.0	5.0	5.1	5.5
	AEQL	256.3	226.5	201.1	228.3	70.3	65.2	66.8	72.3	67.0	63.5	66.3	71.0
0.9	0.2	172.9	178.4	183.8	183.6	99.2	118.6	129.7	130.6	83.3	104.3	116.6	117.7
	0.4	134.2	142.6	147.3	148.1	48.5	57.8	63.0	65.0	39.3	47.3	51.7	55.0
	0.6	99.4	107.6	107.3	111.2	26.9	31.0	33.6	35.6	22.8	25.8	28.0	30.3
	0.8	70.8	77.9	76.2	82.2	17.1	18.9	20.1	21.8	15.4	16.8	17.9	19.0
	1.0	50.1	54.9	53.7	57.2	12.0	13.1	13.8	14.6	11.5	12.3	12.8	13.7
	1.2	36.0	39.4	38.0	41.5	9.1	9.7	10.0	10.8	9.2	9.5	9.9	10.5
	1.4	25.6	27.9	27.1	29.9	7.3	7.6	7.9	8.5	7.6	7.9	8.1	8.6
	1.6	18.8	20.4	20.0	21.9	6.1	6.3	6.5	6.9	6.5	6.6	6.9	7.2
	1.8	13.9	15.0	14.5	16.5	5.2	5.4	5.5	5.9	5.7	5.8	5.9	6.2
	2.0	10.3	11.2	11.1	12.5	4.6	4.7	4.8	5.1	5.1	5.1	5.2	5.5
	AEQL	198.0	215.2	211.0	229.5	61.3	65.7	68.6	73.2	61.4	64.6	67.6	71.3

Table 3. OC ARLs of control charts for different values of σ_δ^2 and ρ under $\lambda_1\sigma$ in slope.

		T^2				MEWMA				MCUSUM			
ρ	λ_1	**0.00**	**0.01**	**0.04**	**0.09**	**0.00**	**0.01**	**0.04**	**0.09**	**0.00**	**0.01**	**0.04**	**0.09**
	0.025	197.7	203.9	198.4	195.0	176.0	184.3	188.8	173.7	167.4	176.1	180.6	168.9
	0.050	187.5	197.9	192.5	184.8	137.5	147.2	149.7	134.1	125.4	132.4	137.5	125.9
	0.075	177.8	193.0	178.5	172.1	101.9	111.5	111.9	98.7	87.4	93.1	98.7	86.9
	0.100	163.5	178.7	165.8	156.7	73.8	81.6	80.2	71.7	61.3	65.5	68.6	62.3
0.0	0.125	147.2	165.9	148.7	141.6	55.1	59.1	59.6	52.8	44.7	47.3	48.8	45.1
	0.150	130.5	149.2	131.4	124.0	41.5	43.8	43.8	40.0	33.3	35.1	36.5	34.2
	0.175	114.1	134.1	114.8	109.1	31.6	33.3	33.8	30.5	26.3	27.5	28.0	26.4
	0.200	100.2	116.6	99.1	93.6	25.4	26.3	26.0	24.5	21.2	22.1	22.4	21.3
	0.225	87.1	103.8	86.6	81.0	20.3	21.3	21.0	19.6	17.7	18.3	18.4	17.5
	0.250	76.4	87.9	74.6	69.6	16.8	17.4	17.4	16.4	14.9	15.5	15.4	15.0
	AEQL	100.6	115.9	100.3	94.6	30.5	32.3	32.2	29.5	25.8	27.1	27.7	26.0
	0.025	198.5	191.7	196.0	195.0	171.2	169.4	179.6	160.3	186.1	161.9	172.0	151.9
	0.050	191.3	182.7	185.7	184.8	136.3	132.8	138.1	123.9	144.8	120.2	125.6	107.1
	0.075	179.2	171.9	167.9	172.1	100.4	99.5	99.5	91.2	102.1	85.6	86.7	75.5
	0.100	166.2	157.9	152.0	156.7	74.0	72.0	71.3	68.0	71.7	61.6	60.0	54.3
0.1	0.125	148.5	141.4	134.6	141.6	54.6	53.9	51.2	50.7	51.5	44.9	43.1	40.2
	0.150	131.7	127.0	117.0	124.0	41.0	40.7	37.9	38.7	38.0	33.8	32.7	31.1
	0.175	114.8	114.3	99.8	109.1	31.5	31.7	29.4	30.2	29.3	26.8	25.2	24.7
	0.200	100.2	99.3	84.0	93.6	25.0	25.2	23.4	24.3	23.2	21.4	20.4	20.4
	0.225	86.5	86.5	72.9	81.0	20.2	20.5	18.9	19.8	19.0	18.0	17.0	17.1
	0.250	74.5	75.2	62.0	69.6	16.9	17.2	15.7	16.6	16.1	15.2	14.5	14.8
	AEQL	100.5	99.0	87.1	94.6	30.3	30.3	28.6	28.8	28.9	26.0	25.1	24.1
	0.025	197.4	197.8	190.6	191.7	187.7	186.9	165.8	156.0	185.3	184.1	157.8	145.6
	0.050	189.8	192.0	181.5	181.2	153.5	155.1	127.7	117.2	145.0	143.8	113.6	100.5
	0.075	179.9	179.1	170.0	164.7	117.3	117.9	94.3	84.7	105.9	104.2	81.1	71.1
	0.100	165.1	166.5	155.1	147.0	85.6	87.2	70.2	62.5	75.2	72.4	58.4	51.1
0.5	0.125	148.6	150.5	139.6	131.8	62.8	64.5	52.3	46.2	54.8	53.4	42.7	38.6
	0.150	132.3	136.5	126.2	116.9	47.1	48.0	40.1	35.7	40.3	39.4	32.9	30.0
	0.175	116.6	119.3	109.6	101.3	36.5	37.0	31.3	28.7	31.3	30.5	26.1	24.2
	0.200	102.7	105.8	95.6	88.0	28.5	29.0	25.0	23.1	24.8	24.4	21.3	19.9
	0.225	89.2	93.2	83.9	77.5	22.8	23.3	20.4	19.0	20.3	20.1	18.0	16.8
	0.250	76.9	80.5	73.9	66.6	18.8	19.4	17.2	16.0	17.0	16.9	15.4	14.5
	AEQL	102.3	105.3	96.6	89.5	34.6	35.3	29.8	27.1	30.5	30.0	25.4	23.3
	0.025	191.0	195.5	197.5	195.5	163.1	169.4	188.4	179.5	153.1	171.0	184.9	171.0
	0.050	180.9	187.4	194.7	187.2	125.0	132.8	161.3	145.2	110.8	127.7	148.6	131.3
	0.075	168.1	177.5	182.3	177.6	93.3	99.5	127.1	109.5	78.8	92.5	110.3	93.3
	0.100	151.3	160.6	170.8	163.2	68.3	72.0	97.2	83.2	56.5	65.9	78.6	69.3
0.9	0.125	136.6	144.8	157.7	150.4	51.5	53.9	72.6	62.6	42.3	48.8	57.7	50.5
	0.150	121.3	130.2	146.6	135.3	39.9	40.7	55.0	48.7	33.0	37.4	43.3	38.8
	0.175	106.9	115.2	130.0	120.6	31.4	31.7	42.9	37.7	26.4	29.0	33.8	29.9
	0.200	93.9	101.0	115.0	106.8	25.4	25.2	33.5	29.7	21.6	23.7	27.2	24.6
	0.225	82.3	87.6	102.9	94.7	21.0	20.5	27.0	24.4	18.3	19.5	22.3	20.3
	0.250	70.5	77.4	90.9	82.5	17.6	17.2	22.2	20.1	15.8	16.5	18.9	17.4
	AEQL	94.0	100.9	114.3	106.1	29.8	30.3	39.9	35.3	25.5	28.3	32.8	29.3

According to Tables 2 and 3, the performance of both OC ARLs and AEQRLs shows that MEWMA and MCUSUM charts perform uniformly better than the T^2 chart at various σ_δ^2 and ρ when monitoring regression parameters. When detecting shifts in the intercept, MCUSUM performs better than MEWMA for a small shift, whereas MEWMA performs slightly better than MCUSUM for a large shift. From Table 3, under different shifts in slope, MCUSUM performs slightly better than MEWMA.

As shown in Table 4, under different shifts in standard deviation, the Hotelling T^2 chart performs significantly better than MEWMA and MCUSUM charts, while MEWMA performs better than MCUSUM at different σ_δ^2 and ρ.

It is evident that σ_δ^2 and the correlation coefficient ρ have little effect on the performance of the proposed methods. MCUSUM and MEWMA control charts perform better than the T^2 chart when a shift occurs in the regression parameters. When a shift occurs in standard deviation, the T^2 chart uniformly performs better than the other two methods.

Table 4. OC ARLs of control charts for different values of σ_δ^2 and ρ under $\gamma\sigma$ in standard deviation.

		T^2				MEWMA				MCUSUM			
ρ	γ	**0.00**	**0.01**	**0.04**	**0.09**	**0.00**	**0.01**	**0.04**	**0.09**	**0.00**	**0.01**	**0.04**	**0.09**
0.0	1.2	67.6	72.2	80.5	87.7	84.7	92.4	95.8	102.7	93.0	101.3	101.1	110.2
	1.4	29.8	32.6	38.0	43.0	44.8	50.5	53.5	59.1	52.3	59.2	59.6	64.5
	1.6	16.4	17.9	21.0	24.6	27.9	32.0	33.8	38.4	33.6	39.7	38.7	42.6
	1.8	10.5	11.4	13.6	15.4	19.5	22.0	23.4	26.6	23.8	27.8	27.5	30.1
	2.0	7.5	8.1	9.4	10.9	14.8	16.3	17.3	19.6	18.0	21.2	20.8	22.8
	2.2	5.8	6.1	7.1	8.2	11.4	12.7	13.6	15.3	14.4	16.9	16.3	18.1
	2.4	4.7	5.0	5.7	6.3	9.5	10.4	11.0	12.3	11.7	13.8	13.3	14.7
	2.6	4.0	4.3	4.7	5.3	7.9	8.7	9.2	10.3	10.0	11.6	11.3	12.2
	2.8	3.5	3.6	4.1	4.4	6.8	7.4	7.8	8.8	8.5	9.9	9.6	10.6
	3.0	3.1	3.2	3.6	3.9	5.9	6.6	6.8	7.7	7.5	8.7	8.5	9.0
	AEQL	39.6	42.0	47.9	53.8	74.5	82.5	87.2	97.8	92.2	107.2	104.8	114.2
0.1	1.2	74.0	68.1	94.3	81.6	90.2	75.2	109.1	100.9	97.2	91.3	112.8	110.8
	1.4	33.1	29.9	45.8	39.5	48.8	40.4	62.2	57.5	54.5	51.0	68.4	68.6
	1.6	18.4	16.7	25.3	22.2	30.0	24.5	39.3	37.0	35.6	33.3	45.1	46.2
	1.8	11.5	10.7	15.6	14.2	20.8	17.2	27.0	25.9	25.2	23.6	32.4	33.0
	2.0	8.2	7.7	10.8	10.0	15.3	12.6	19.9	19.5	19.3	17.7	24.4	25.3
	2.2	6.2	6.0	8.0	7.6	12.1	9.9	15.4	15.2	15.1	14.2	19.4	19.8
	2.4	5.0	4.8	6.3	6.1	10.0	8.2	12.5	12.1	12.4	11.5	15.6	16.4
	2.6	4.3	4.1	5.3	5.0	8.3	6.9	10.3	10.2	10.5	9.7	13.1	13.8
	2.8	3.6	3.5	4.4	4.3	7.1	5.9	8.8	8.7	9.0	8.4	11.4	11.9
	3.0	3.2	3.2	3.8	3.7	6.2	5.1	7.6	7.5	7.8	7.3	9.8	10.2
	AEQL	42.3	40.3	53.8	50.5	78.6	64.7	98.7	96.2	97.0	90.4	122.6	126.9
0.5	1.2	70.6	70.9	79.3	90.2	87.7	88.3	89.8	109.7	92.7	95.5	90.9	116.0
	1.4	31.7	31.3	37.4	44.1	46.4	47.2	49.4	64.0	51.7	54.3	53.1	71.9
	1.6	17.3	17.5	20.5	25.1	29.4	29.5	31.1	40.5	32.5	35.4	34.8	47.5
	1.8	11.1	11.2	13.0	15.9	19.9	20.3	21.5	28.0	23.0	25.0	24.5	34.1
	2.0	7.8	8.0	9.1	11.2	14.8	15.3	16.0	20.9	17.3	19.0	18.3	26.2
	2.2	6.1	6.1	6.9	8.2	11.8	12.0	12.6	16.2	13.7	15.2	14.6	20.5
	2.4	4.9	5.0	5.6	6.5	9.6	9.8	10.3	13.1	11.3	12.2	11.9	16.8
	2.6	4.1	4.2	4.6	5.3	7.9	8.2	8.7	10.9	9.5	10.5	9.9	13.9
	2.8	3.6	3.7	4.0	4.5	6.9	7.1	7.4	9.3	8.1	9.0	8.5	11.9
	3.0	3.2	3.2	3.5	3.9	6.1	6.2	6.6	8.0	7.1	7.9	7.6	10.4
	AEQL	41.1	41.6	46.8	54.8	75.9	77.6	81.9	103.3	88.3	96.7	93.0	129.8
0.9	1.2	68.2	72.7	81.3	97.0	89.7	78.3	95.6	111.2	101.0	97.3	104.9	116.5
	1.4	29.5	32.6	37.7	49.0	47.1	41.3	53.3	64.9	58.3	55.6	62.1	70.9
	1.6	16.2	17.7	20.5	27.6	29.3	25.5	33.2	41.7	37.5	36.0	40.3	47.5
	1.8	10.4	11.3	13.1	17.2	20.6	17.2	23.1	28.9	26.4	25.6	28.7	34.6
	2.0	7.5	8.0	9.3	12.0	15.2	12.8	17.2	21.3	20.0	19.4	21.9	25.7
	2.2	5.8	6.2	7.1	8.8	12.1	10.2	13.3	16.4	15.8	15.3	17.5	20.6
	2.4	4.7	4.9	5.6	7.0	9.8	8.3	11.0	13.3	13.1	12.6	14.3	16.8
	2.6	4.0	4.1	4.7	5.7	8.2	7.0	9.1	11.1	11.0	10.6	12.0	14.1
	2.8	3.5	3.6	4.0	4.8	7.1	6.0	7.8	9.5	9.5	9.2	10.3	12.2
	3.0	3.1	3.2	3.5	4.1	6.2	5.3	6.8	8.1	8.3	8.0	9.0	10.4
	AEQL	39.6	41.7	47.3	58.8	77.6	66.1	86.3	105.4	102.1	98.8	111.2	130.4

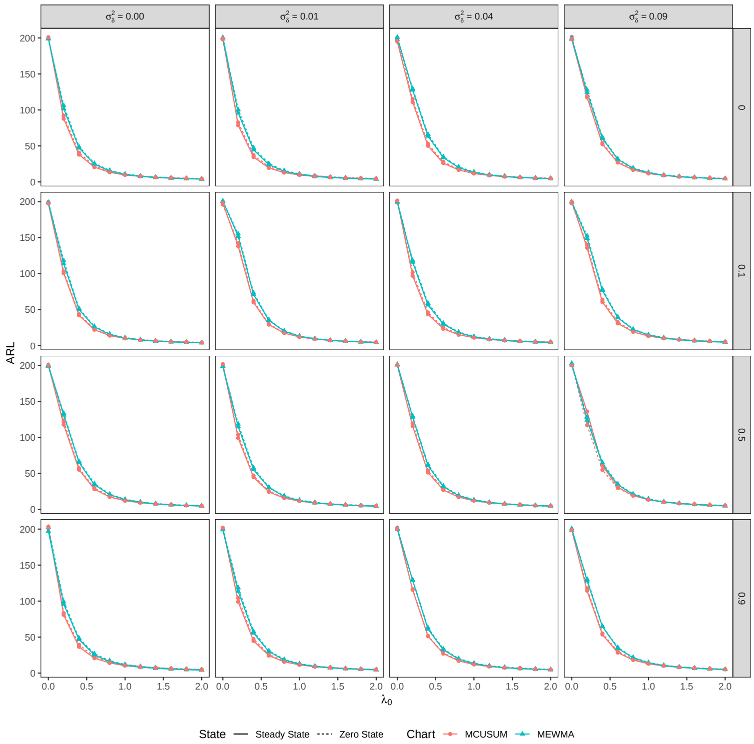

Figure 1. Zero-state and steady-state ARL for MCUSUM and MEWMA under shift in intercept.

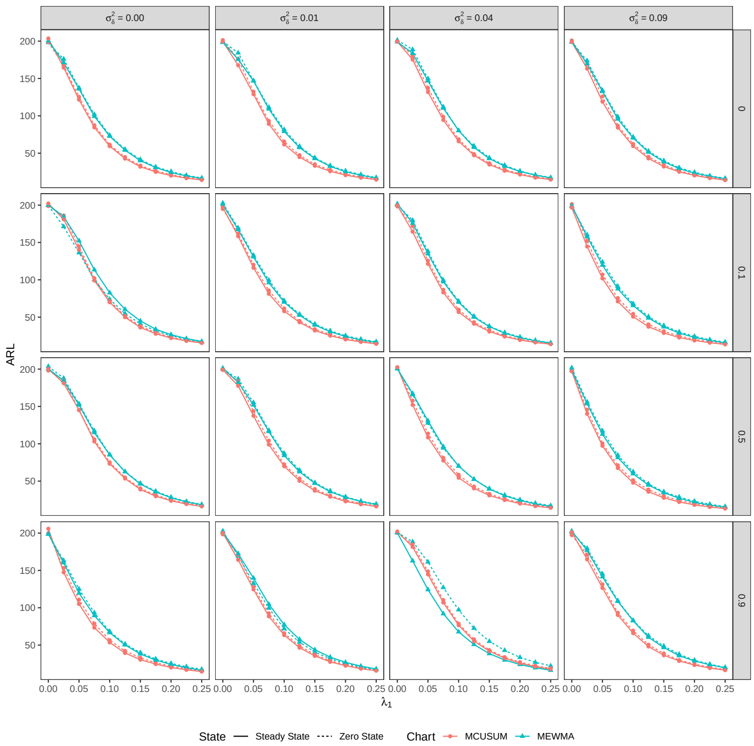

Figure 2. Zero-state and steady-state ARL for MCUSUM and MEWMA under shift in slope.

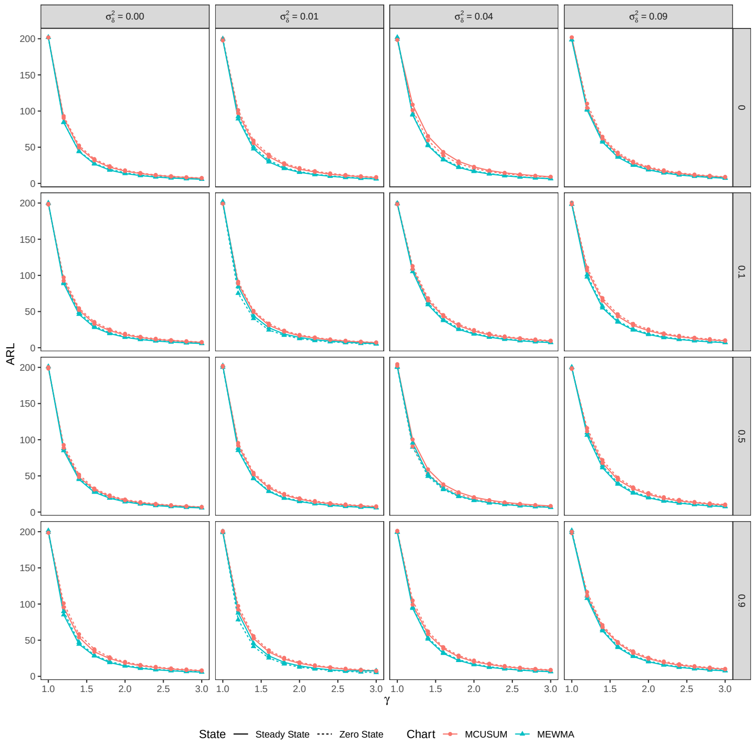

Figure 3. Zero-state and steady-state ARL for MCUSUM and MEWMA under shift in standard deviation.

Effect of Ignoring Measurement Error and/or Random Effects

In this section, we evaluate the effect of an absence of measurement errors and/or random effects within the profile. We use the MCUSUM statistic as an example.

When measurement errors are neglected, by substituting $\mathbf{X}_i$ for $\boldsymbol{\xi}_i$ in Equation (3), we obtain an estimate of fixed effects. Then the estimation of $\boldsymbol{\beta}$ for each sample is

$$\hat{\boldsymbol{\beta}}_{i,\mathrm{LMM}} = (\mathbf{X}_i^\top \mathbf{V}_i^{-1}\mathbf{X}_i)^{-1}\mathbf{X}_i^\top \mathbf{V}_i^{-1}\mathbf{Y}_i.$$

Narvand et al. [27] used $\hat{\boldsymbol{\beta}}_{i,\mathrm{LMM}}$ to monitor an LMM model. The MCUSUM LMM is given by

$$\mathbf{s}_i = \begin{cases} \mathbf{0}; & \text{for } c_i \le c, \\ \left(\mathbf{u}_{i-1} + \hat{\boldsymbol{\beta}}_{i,\mathrm{LMM}} - \boldsymbol{\beta}_0\right)(1 - c/c_i); & \text{for } c_i > c, \end{cases}$$

$$c_i = \left[(\mathbf{u}_{i-1} + \hat{\boldsymbol{\beta}}_{i,\mathrm{LMM}} - \boldsymbol{\beta}_0)^\top \hat{\boldsymbol{\Sigma}}_{i,\mathrm{LMM}}^{-1}(\mathbf{u}_{i-1} + \hat{\boldsymbol{\beta}}_{i,\mathrm{LMM}} - \boldsymbol{\beta}_0)\right]^{1/2},$$

where $\mathbf{s}_0 = \mathbf{0}$ and $\hat{\boldsymbol{\Sigma}}_{i,\mathrm{LMM}} = (\mathbf{X}_i^\top \mathbf{V}_i^{-1}\mathbf{X}_i)^{-1}$. When $(\mathbf{s}_i^\top \hat{\boldsymbol{\Sigma}}_{i,\mathrm{LMM}}^{-1}\mathbf{s}_i)^{1/2} > \mathrm{UCL}$, the chart alarms.

When measurement errors and random effects are ignored, one can also use the LS approach to obtain the estimation of fixed effects even though the data follows an LMMeM. That is, the estimation of $\boldsymbol{\beta}$ for each sample is

$$\hat{\boldsymbol{\beta}}_{i,\mathrm{LS}} = (\mathbf{X}_i^\top \mathbf{X}_i)^{-1}\mathbf{X}_i^\top \mathbf{Y}_i.$$

The MCUSUM LS statistic is modified as follows.

$$\mathbf{s}_i = \begin{cases} \mathbf{0}; & \text{for } c_i \le c, \\ \left(\mathbf{u}_{i-1} + \hat{\boldsymbol{\beta}}_{i,\mathrm{LS}} - \boldsymbol{\beta}_0\right)(1 - c/c_i); & \text{for } c_i > c, \end{cases}$$

$$c_i = \left[(\mathbf{u}_{i-1} + \hat{\boldsymbol{\beta}}_{i,\mathrm{LS}} - \boldsymbol{\beta}_0)^\top \hat{\boldsymbol{\Sigma}}_{i,\mathrm{LS}}^{-1}(\mathbf{u}_{i-1} + \hat{\boldsymbol{\beta}}_{i,\mathrm{LS}} - \boldsymbol{\beta}_0)\right]^{1/2},$$

where $\mathbf{s}_0 = \mathbf{0}$ and $\hat{\boldsymbol{\Sigma}}_{i,\mathrm{LS}} = (\mathbf{X}_i^\top \mathbf{X}_i)^{-1}$. When $(\mathbf{s}_i^\top \hat{\boldsymbol{\Sigma}}_{i,\mathrm{LS}}^{-1}\mathbf{s}_i)^{1/2} > \mathrm{UCL}$, the chart alarms.

All the control limits are calculated as described in Section 3.5 to yield IC ARL of approximately 200. The comparison results are presented in Figures 4–6. "MCUSUM LMMeM" in the legend represents our proposed MCUSUM control chart.

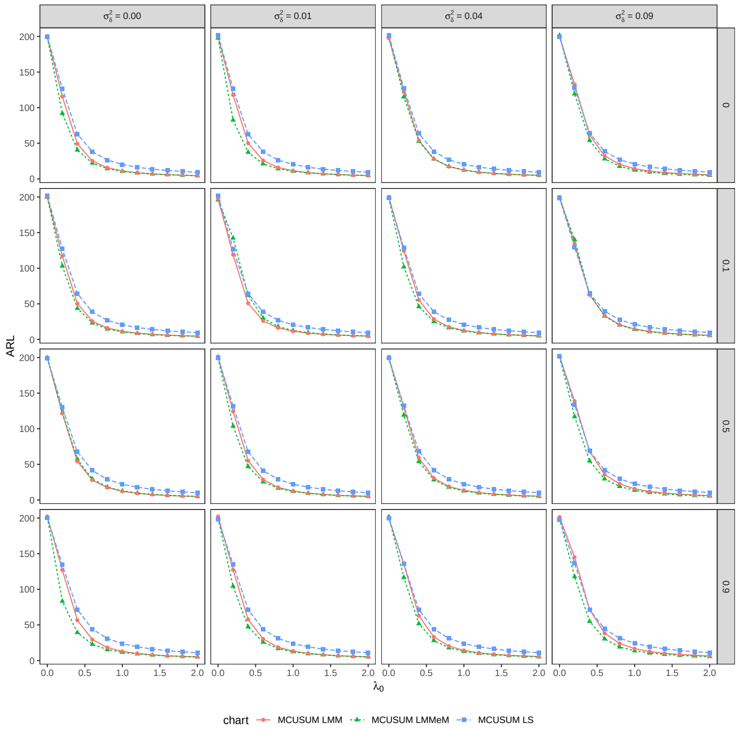

Figure 4. Effect of ignoring measurement errors and/or random effects on ARL performance for MCUSUM control charts under different shifts in intercept.

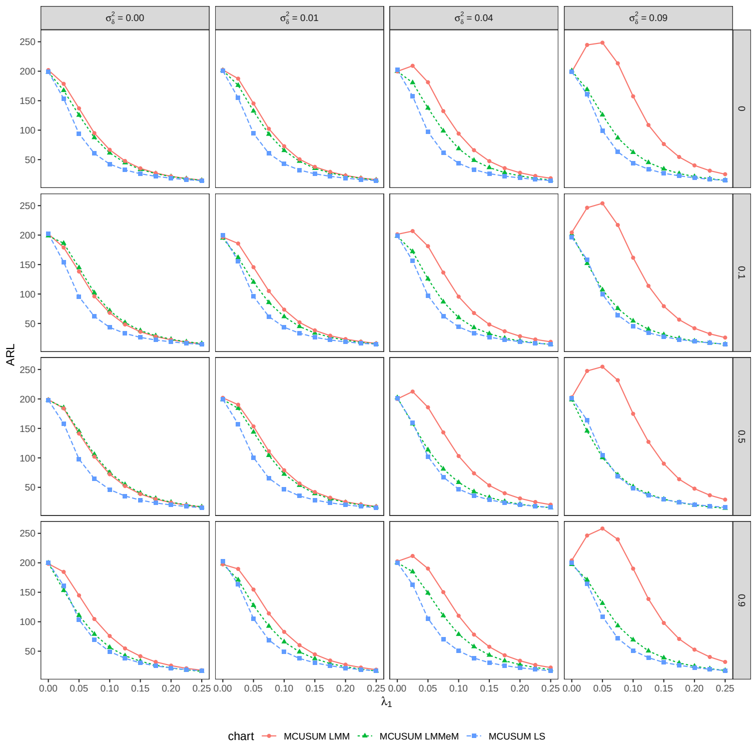

Figure 5. Effect of ignoring measurement errors and/or random effects on ARL performance for MCUSUM control charts under different shifts in slope.

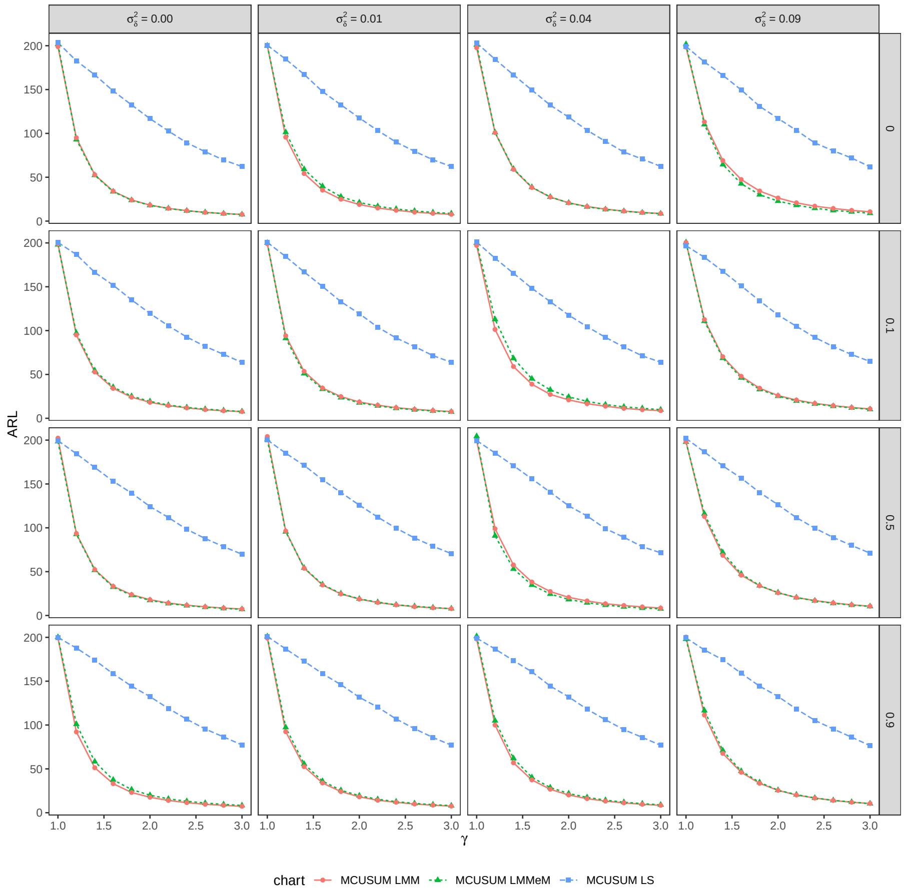

Figure 6. Effect of ignoring measurement errors and random effects on ARL performance for MCUSUM control chart under different shifts in standard deviation.

From Figure 4, for any shifts in the intercept, our method performs slightly better than the MCUSUM LMM and MCUSUM LS methods. According to Figure 5, when the slope term of fixed effect occurs as a step shift, MCUSUM LMM performs worst when the measurement errors increased and even fails to alarm in detecting small shifts. Our control chart performs slightly worse than the MCUSUM LS chart that ignores any measurement errors and random effects. The MCUSUM LMM scheme performs relatively similar to our chart with various measurements in detecting a shift in σ, while MCUSUM LS performs worst among all three of the charts.

Based on the above analysis, ignoring measurement errors will reduce the performance of the MCUSUM chart in detecting shifts in regression parameters, and ignoring measurement errors and random effects will decrease the performance of the MCUSUM chart in monitoring intercept terms of fix effects or standard deviation.

5. Case Study

In this section, 150 healthcare expenditures (in million EUR) randomly selected from 15 regions (Austria, Belgium, Cyprus, Denmark, Estonia, Finland, France, Germany, Greece, Hungary, Lithuania, Netherlands, Portugal, Spain, and Switzerland) which were regularly obtained during the period 2010–2019, inclusive, are used in our real data analysis. The data are available from the official Eurostat website https://ec.europa.eu/eurostat (acceaaed on 16 May 2022).

We define the response as healthcare expenditures, which are declared in logarithm with the fixed effect set as the infant mortality rate (IMR). Figure 7 presents a simple linear regression plot of the healthcare expenditures versus IMR for each region.

We are interested in a linear mixed measurement effects model for the data:

$$y_{ki} = \beta_0 + \beta_1 \xi_{ki} + b_{0i} + b_{1i} z_{ki} + \varepsilon_{ki},$$
$$x_{ki} = \xi_{ki} + \delta_{ki}, \quad k = 1, \ldots, 10, i = 1, \ldots, 15,$$

where y_{ki} indicates the kth observation of the ith region of the response, x_{ki} indicates the kth observation of the ith region of the explanatory variable IMR, and $z_{ki} = k - 1$ is a time variable (from 0 to 9).

Based on the preceding analysis, we have $\hat{\sigma}_\delta^2 = 0.168$, $\hat{\boldsymbol{\beta}}_c = (10.466, -0.0104)^\top$, $\hat{\sigma}^2 = 0.0018$ and

$$\hat{\mathbf{D}} = \begin{pmatrix} 3.0786 & -0.0255 \\ -0.0255 & 0.0014 \end{pmatrix}.$$

We then apply the MCUSUM, MEWMA, and T^2 charts to monitor the random effects of the above LMMeM. The smoothing constants for MCUSUM and MEWMA are set to 0.5 and 0.2, respectively. The UCLs for proposed charts are searched based on 20,000 simulated replicates to generate an IC ARL of approximately 200. In order to check the performance of the proposed charts, eight in-control and seven out-of-control data under the 0.8 shift in intercept consecutively are generated. The control charts are presented in Figure 8.

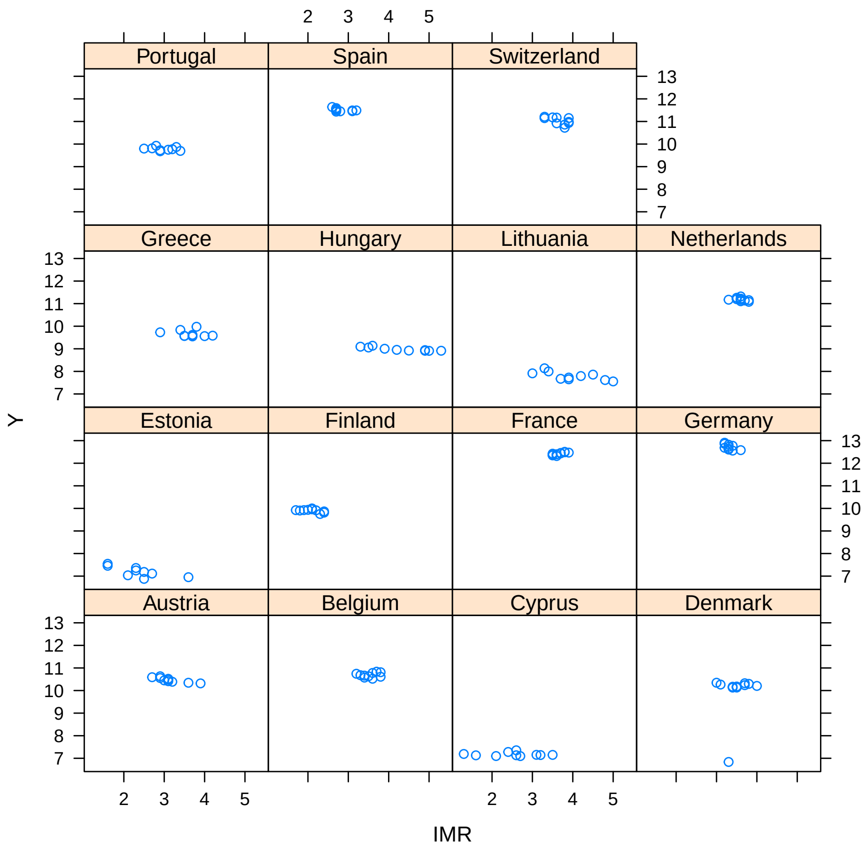

Figure 7. Healthcare expenditures versus IMR.

As we can see from Figure 8, the MCUSUM, MEWMA, and T^2 charts can quickly detect the OC condition in the 9th, 9th, and 10th samples, respectively.

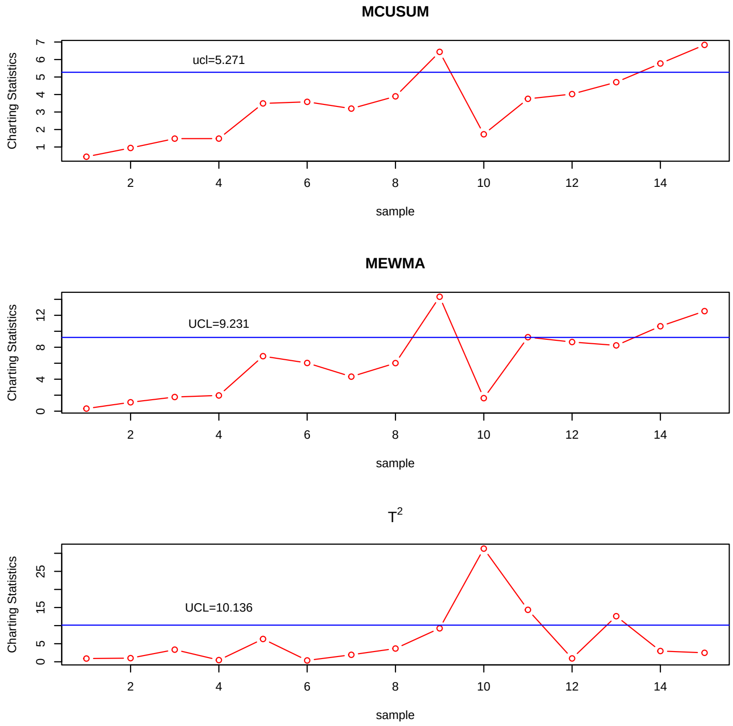

Figure 8. MCUSUM, MEWMA, and T^2 control charts under intercept shift coefficient of 0.8.

6. Conclusions

In this paper, we extend the work of [28] to apply a linear mixed model to the situation where the fixed effects are subject to measurement errors. Simulation studies show that ignoring measurement errors and/or random effects can severely decrease the performance of the control charts. For monitoring an LMMeM, T^2 chart performs best among the three charts for detecting shifts in process standard deviation, but has the worst performance for detecting shifts in the regression parameters. Under the shifts in the intercept, MCUSUM performs better than MEWMA for small shifts, whereas MEWMA performs slightly better than MCUSUM for large shifts, and MCUSUM outperforms MEWMA overall. MCUSUM is the preferred chart among the three charts for detecting shifts in slope while MEWMA performs better than MCUSUM for shifts in the standard deviation.

Author Contributions: Methodology, W.L., Z.L. and Z.W.; formal analysis, W.L.; writing—original draft preparation, W.L.; writing—review and editing, W.L. and Z.L. All authors have read and agreed to the published version of the manuscript.

Funding: This work is supported by the National Natural Science Foundation (NNSF) of China under Grants 11971247 and 12071233.

Data Availability Statement: The data are available from the official Eurostat website https://ec.europa.eu/eurostat.

Conflicts of Interest: The authors declare no conflicts of interest.

Appendix A. Estimation of D and σ^2

In practice, **D** and σ^2 are unknown and we need to use historical data to estimate them. Inspired by [56], we consider the following two-step iterative procedure to estimate the fixed and random effects. We start with the initial values

$$\hat{\beta} = \hat{\beta}^{(0)} = \left(\sum_{i=1}^{m} \mathbf{X}_i^\top \mathbf{X}_i - n\boldsymbol{\Lambda} \right)^{-1} \left(\sum_{i=1}^{m} \mathbf{X}_i^\top \mathbf{Y}_i \right).$$

Step 1: Predict the residuals given $\hat{\beta}_c$ for subject i,

$$\mathbf{u}_i = \mathbf{Y}_i - \mathbf{X}_i \hat{\beta}_c,$$

for $i = 1, \ldots, m$. We can estimate

$$\hat{\mathbf{b}}_i = \left(\mathbf{Z}_i^\top \mathbf{Z}_i\right)^{-1} \mathbf{Z}_i^\top \mathbf{u}_i$$

and residual $e_i = \mathbf{u}_i - \mathbf{Z}_i \hat{\mathbf{b}}_i$. Based on $\mathbf{e}_i$ and $\hat{\mathbf{b}}_i$, we propose an estimator of σ^2,

$$\hat{\sigma}^2 = \max\left\{0, \frac{1}{(n - qm)} \sum_{i=1}^{m} e_i^\top \mathbf{e}_i - \hat{\beta}_c^\top \boldsymbol{\Lambda} \hat{\beta}_c \right\}.$$

We will derive the estimation equation of $\mathbf{D}$. From the estimator of $\mathbf{b}_i$, we can see

$$\hat{\mathbf{b}}_i = \left(\mathbf{Z}_i^\top \mathbf{Z}_i\right)^{-1} \mathbf{Z}_i^\top \mathbf{u}_i = \mathbf{b}_i + \left(\mathbf{Z}_i^\top \mathbf{Z}_i\right)^{-1} \mathbf{Z}_i^\top \varepsilon_i.$$

This leads to

$$\begin{aligned} \sum_{i=1}^{m} \mathbf{b}_i \mathbf{b}_i^\top = & \sum_{i=1}^{m} \hat{\mathbf{b}}_i \hat{\mathbf{b}}_i^\top + \sum_{i=1}^{m} \left(\mathbf{Z}_i^\top \mathbf{Z}_i\right)^{-1} \mathbf{Z}_i^\top \varepsilon_i \varepsilon_i^\top \mathbf{Z}_i \left(\mathbf{Z}_i^\top \mathbf{Z}_i\right)^{-1} \\ & + \sum_{i=1}^{m} \left(\mathbf{Z}_i^\top \mathbf{Z}_i\right)^{-1} \mathbf{Z}_i^\top \varepsilon_i \mathbf{b}_i^\top + \sum_{i=1}^{m} \mathbf{b}_i \varepsilon_i^\top \mathbf{Z}_i \left(\mathbf{Z}_i^\top \mathbf{Z}_i\right)^{-1}. \end{aligned}$$

As [56] pointed out, the last two terms are of order $Op\left(m^{1/2}\right)$, hence

$$\begin{aligned} \frac{1}{m} \sum_{i=1}^{m} \mathbf{b}_i \mathbf{b}_i^\top & \approx \frac{1}{m} \left\{ \sum_{i=1}^{m} \hat{\mathbf{b}}_i \hat{\mathbf{b}}_i^\top - \sum_{i=1}^{m} \left(\mathbf{Z}_i^\top \mathbf{Z}_i\right)^{-1} \mathbf{Z}_i^\top \varepsilon_i \varepsilon_i^\top \mathbf{Z}_i \left(\mathbf{Z}_i^\top \mathbf{Z}_i\right)^{-1} \right\} \\ & \approx \frac{1}{m} \left\{ \sum_{i=1}^{m} \hat{\mathbf{b}}_i \hat{\mathbf{b}}_i^\top - \sum_{i=1}^{m} (\hat{\sigma}^2 + \hat{\beta}_c^\top \boldsymbol{\Lambda} \hat{\beta}_c) \left(\mathbf{Z}_i^\top \mathbf{Z}_i\right)^{-1} \right\}. \end{aligned}$$

Correspondingly,

$$\hat{\mathbf{D}} = \frac{1}{m} \sum_{i=1}^{m} \hat{\mathbf{b}}_i \hat{\mathbf{b}}_i^\top - \frac{1}{m} (\hat{\sigma}^2 + \hat{\beta}_c^\top \boldsymbol{\Lambda} \hat{\beta}_c) \sum_{i=1}^{m} \left(\mathbf{Z}_i^\top \mathbf{Z}_i\right)^{-1}.$$

Step 2: Given $\mathbf{D}$, we can update the estimate of $\mathbf{D}$ by

$$\hat{\beta}_c = \left(\sum_{i=1}^{m} \mathbf{X}_i^\top \hat{\mathbf{V}}_i^{-1} \mathbf{X}_i - \mathrm{tr}(\hat{\mathbf{V}}_i^{-1}) \boldsymbol{\Lambda} \right)^{-1} \left(\sum_{i=1}^{m} \mathbf{X}_i^\top \mathbf{V}_i^{-1} \mathbf{Y}_i \right),$$

where $\hat{\mathbf{V}}_i = \mathbf{Z}_i \hat{\mathbf{D}} \mathbf{Z}_i^\top + \hat{\sigma}^2 \mathbf{I}_n$.

To achieve numerically stable estimates of $\hat{\sigma}^2$, $\hat{\beta}_c$, and $\hat{\mathbf{D}}$, we can iterate between Step 1 and Step 2 until convergence.

References

1. Kang, L.; Albin, S.L. On-line monitoring when the process yields a linear profile. *J. Qual. Technol.* **2000**, *32*, 418–426. [CrossRef]
2. Woodall, W.H.; Spitzner, D.J.; Montgomery, D.C.; Gupta, S. Using Control Charts to Monitor Process and Product Quality Profiles. *J. Qual. Technol.* **2004**, *36*, 309–320. [CrossRef]
3. Maleki, M.R.; Amiri, A.; Castagliola, P. An overview on recent profile monitoring papers (2008–2018) based on conceptual classification scheme. *Comput. Ind. Eng.* **2018**, *126*, 705–728. [CrossRef]
4. Stover, F.S.; Brill, R.V. Statistical quality control applied to ion chromatography calibrations. *J. Chromatogr. A* **1998**, *804*, 37–43. [CrossRef]

5. Kim, K.; Mahmoud, M.A.; Woodall, W.H. On the monitoring of linear profiles. *J. Qual. Technol.* **2003**, *35*, 317–328. [CrossRef]
6. Mahmoud, M.A.; Woodall, W.H. Phase I analysis of linear profiles with calibration applications. *Technometrics* **2004**, *46*, 380–391. [CrossRef]
7. Zou, C.; Zhang, Y.; Wang, Z. A control chart based on a change-point model for monitoring linear profiles. *IIE Trans.* **2006**, *38*, 1093–1103. [CrossRef]
8. Mahmoud, M.A.; Parker, P.A.; Woodall, W.H.; Hawkins, D.M. A change point method for linear profile data. *Qual. Reliab. Eng. Int.* **2007**, *23*, 247–268. [CrossRef]
9. Zhang, J.; Li, Z.; Wang, Z. Control chart based on likelihood ratio for monitoring linear profiles. *Comput. Stat. Data Anal.* **2009**, *53*, 1440–1448. [CrossRef]
10. Li, Z.; Wang, Z. An exponentially weighted moving average scheme with variable sampling intervals for monitoring linear profiles. *Comput. Ind. Eng.* **2010**, *59*, 630–637. [CrossRef]
11. Amiri, A.; Mehrjoo, M.; Pasek, Z.J. Modifying simple linear profiles monitoring schemes in phase II to detect decreasing step shifts and drifts. *Int. J. Adv. Manuf. Technol.* **2013**, *64*, 1323–1332. [CrossRef]
12. Kazemzadeh, R.B.; Noorossana, R.; Amiri, A. Phase I monitoring of polynomial profiles. *Commun. Stat. Theory Methods* **2008**, *37*, 1671–1686. [CrossRef]
13. Kazemzadeh, R.; Noorossana, R.; Amiri, A. Monitoring polynomial profiles in quality control applications. *Int. J. Adv. Manuf. Technol.* **2009**, *42*, 703–712. [CrossRef]
14. Zou, C.; Tsung, F.; Wang, Z. Monitoring general linear profiles using multivariate exponentially weighted moving average schemes. *Technometrics* **2007**, *49*, 395–408. [CrossRef]
15. Mahmoud, M.A. Phase I analysis of multiple linear regression profiles. *Commun. Stat. Simul. Comput.* **2008**, *37*, 2106–2130. [CrossRef]
16. Noorossana, R.; Eyvazian, M.; Vaghefi, A. Phase II monitoring of multivariate simple linear profiles. *Comput. Ind. Eng.* **2010**, *58*, 563–570. [CrossRef]
17. Zi, X.; Zou, C.; Tsung, F. A distribution-free robust method for monitoring linear profiles using rank-based regression. *IIE Trans.* **2012**, *44*, 949–963. [CrossRef]
18. Zou, C.; Ning, X.; Tsung, F. LASSO-based multivariate linear profile monitoring. *Ann. Oper. Res.* **2012**, *192*, 3–19. [CrossRef]
19. Ding, Y.; Zeng, L.; Zhou, S. Phase I analysis for monitoring nonlinear profiles in manufacturing processes. *J. Qual. Technol.* **2006**, *38*, 199–216. [CrossRef]
20. Moguerza, J.M.; Muñoz, A.; Psarakis, S. Monitoring nonlinear profiles using support vector machines. In *Proceedings of the Progress in Pattern Recognition, Image Analysis and Applications*; Springer: Berlin/Heidelberg, Germany, 2007; pp. 574–583. [CrossRef]
21. Williams, J.D.; Woodall, W.H.; Birch, J.B. Statistical monitoring of nonlinear product and process quality profiles. *Qual. Reliab. Eng. Int.* **2007**, *23*, 925–941. [CrossRef]
22. Vaghefi, A.; Tajbakhsh, S.D.; Noorossana, R. Phase II monitoring of nonlinear profiles. *Commun. Stat. Theory Methods* **2009**, *38*, 1834–1851. [CrossRef]
23. Fan, S.K.S.; Chang, Y.J.; Aidara, N. Nonlinear profile monitoring of reflow process data based on the sum of sine functions. *Qual. Reliab. Eng. Int.* **2013**, *29*, 743–758. [CrossRef]
24. Xin, H.; Hsieh, W.J.; Lio, Y.; Tsai, T.R. Nonlinear Profile Monitoring Using Spline Functions. *Mathematics* **2020**, *8*, 1588. [CrossRef]
25. Jensen, W.A.; Birch, J.B.; Woodall, W.H. Monitoring correlation within linear profiles using mixed models. *J. Qual. Technol.* **2008**, *40*, 167–183. [CrossRef]
26. Jensen, W.A.; Birch, J.B. Profile monitoring via nonlinear mixed models. *J. Qual. Technol.* **2009**, *41*, 18–34. [CrossRef]
27. Narvand, A.; Soleimani, P.; Raissi, S. Phase II monitoring of auto-correlated linear profiles using linear mixed model. *J. Ind. Eng. Int.* **2013**, *9*, 1–9. [CrossRef]
28. Soleimani, P.; Narvand, A.; Raissi, S. Online monitoring of auto correlated linear profiles via mixed model. *Int. J. Manuf. Technol. Manag.* **2013**, *27*, 238–250. [CrossRef]
29. Maleki, M.R.; Amiri, A.; Castagliola, P. Measurement errors in statistical process monitoring: A literature review. *Comput. Ind. Eng.* **2017**, *103*, 316–329. [CrossRef]
30. Linna, K.W.; Woodall, W.H. Effect of measurement error on Shewhart control charts. *J. Qual. Technol.* **2001**, *33*, 213–222. [CrossRef]
31. Linna, K.W.; Woodall, W.H.; Busby, K.L. The performance of multivariate control charts in the presence of measurement error. *J. Qual. Technol.* **2001**, *33*, 349–355. [CrossRef]
32. Maravelakis, P.; Panaretos, J.; Psarakis, S. EWMA chart and measurement error. *J. Appl. Stat.* **2004**, *31*, 445–455. [CrossRef]
33. Tran, K.P.; Castagliola, P.; Celano, G. The performance of the Shewhart-RZ control chart in the presence of measurement error. *Int. J. Prod. Res.* **2016**, *54*, 7504–7522. [CrossRef]
34. Chen, L.P.; Yang, S.F. A New p-Control Chart with Measurement Error Correction. *arXiv* **2022**, arXiv:2203.03384.
35. Li, J.; Huang, S. Regression-based process monitoring with consideration of measurement errors. *IIE Trans.* **2009**, *42*, 146–160. [CrossRef]
36. Wang, Y.H.T.; Huwang, L. On the monitoring of simple linear Berkson profiles. *Qual. Reliab. Eng. Int.* **2012**, *28*, 949–965. [CrossRef]
37. Noorossana, R.; Zerehsaz, Y. Effect of measurement error on phase II monitoring of simple linear profiles. *Int. J. Adv. Manuf. Technol.* **2015**, *79*, 2031–2040. [CrossRef]

38. Deaton, A. Panel data from time series of cross-sections. *J. Econom.* **1985**, *30*, 109–126. [CrossRef]
39. Fuller, W.A. *Measurement Error Models*; Wiley: New York, NY, USA, 1987. [CrossRef]
40. Cheng, C.L.; Van Ness, J.W. *Statistical Regression with Measurement Error*; Arnold: London, UK, 1999.
41. Carroll, R.J.; Ruppert, D.; Stefanski, L.A.; Crainiceanu, C.M. *Measurement Error in Nonlinear Models: A Modern Perspective*; Chapman and Hall/CRC: Boca Raton, FL, USA, 2006. [CrossRef]
42. Buonaccorsi, J.P. *Measurement Error: Models, Methods, and Applications*; Chapman and Hall/CRC: Boca Raton, FL, USA, 2010. [CrossRef]
43. Liu, J.; Chen, X. Consistency of LS estimator in simple linear EV regression models. *Acta Math. Sci.* **2005**, *25*, 50–58. [CrossRef]
44. Miao, Y.; Zhao, F.; Wang, K. Central limit theorems for LS estimators in the EV regression model with dependent measurements. *J. Korean Stat. Soc.* **2011**, *40*, 303–312. [CrossRef]
45. Xu, S.; Li, N. Consistency for the LS estimator in the linear EV regression model with replicate observations. *J. Korean Stat. Soc.* **2013**, *42*, 451–458. [CrossRef]
46. Harville, D.A. Maximum likelihood approaches to variance component estimation and to related problems. *J. Am. Stat. Assoc.* **1977**, *72*, 320–338. [CrossRef]
47. Zhong, X.; Fung, W.; Wei, B. Estimation in linear models with random effects and errors-in-variables. *Ann. Inst. Statist. Math.* **2002**, *54*, 595–606. [CrossRef]
48. Sullivan, J.H.; Woodall, W.H. A comparison of multivariate control charts for individual observations. *J. Qual. Technol.* **1996**, *28*, 398–408. [CrossRef]
49. Fung, W.K.; Zhong, X.P.; Wei, B.C. On estimation and influence diagnostics in linear mixed measurement error models. *AJMMS-Am. J. Math. Manag. Sci.* **2003**, *23*, 37–59. [CrossRef]
50. Zare, K.; Rasekh, A. Diagnostic measures for linear mixed measurement error models. *SORT-Stat. Oper. Res. Trans.* **2011**, *35*, 125–144.
51. Maksaei, N.; Rasekh, A.; Babadi, B. Influence measures and outliers detection in linear mixed measurement error models with Ridge estimation. *Commun. Stat. Simul. Comput.* **2021**, *4*, 1–17. [CrossRef]
52. Yavarizadeh, B.; Rasekh, A.; Ahmed, S.E.; Babadi, B. Ridge estimation in linear mixed measurement error models with stochastic linear mixed restrictions. *Commun. Stat. Simul. Comput.* **2022**, *51*, 3037–3053. [CrossRef]
53. Lowry, C.A.; Woodall, W.H.; Champ, C.W.; Rigdon, S.E. A multivariate exponentially weighted moving average control chart. *Technometrics* **1992**, *34*, 46–53. [CrossRef]
54. Crosier, R.B. Multivariate generalizations of cumulative sum quality-control schemes. *Technometrics* **1988**, *30*, 291–303. [CrossRef]
55. Montgomery, D.C. *Introduction to Statistical Quality Control*; John Wiley & Sons: New York, NY, USA, 2005.
56. Sun, Y.; Zhang, W.; Tong, H. Estimation of the covariance matrix of random effects in longitudinal studies. *Ann. Statist.* **2007**, *35*, 2795–2814. [CrossRef]